Resolution of *trans*-1-(2-Naphthyl)-2-phenylethene Fluorescence in the Presence of Tri-*n*-butylamine into Pairs of Monomer and Exciplex Spectra. Selectivity in Conformer Quenching

J. Saltiel,* J.-O. Choi, D. F. Sears, Jr., D. W. Eaker, K. E. O'Shea,† and I. Garcia†

Contribution from the Department of Chemistry, The Florida State University, Tallahassee, Florida 32306-3006

Received April 23, 1996[⊗]

Abstract: Fluorescence spectra of *trans*-1-(2-naphthyl)-2-phenylethene (NPE) obtained at different excitation wavelengths and tri-*n*-butylamine (TBA) concentrations in methylcyclohexane are resolved into four distinct components by application of principal component analysis with self-modeling. Two of the components are the NPE conformer fluorescence spectra, and the other two are the corresponding NPE·TBA exciplexes. Pure component combination coefficients are based on optimization of global (λ_{exc}-independent) Stern−Volmer plots for the monomers and exciplex fluorescence plots for the exciplexes. Conformer-specific fluorescence quenching rate constants by the amine are obtained for the first time. These are indistinguishable from the corresponding exciplex formation rate constants. Fortuitously, the Stern−Volmer constants for the two singlet excited conformer/TBA interactions differ by only ∼25%, revealing high conformer selectivity by TBA. This selectivity is consistent with the large shift between the λ_{max} of the two exciplex fluorescence spectra which reveals the more favorable (2.9 kcal/mol) reduction potential of NPE_A, the less extended conformer.

Quenching of aromatic hydrocarbon fluorescence by amines is a well-documented phenomenon. When singlet excitation transfer is energetically unfavorable, the amine functions as the electron donor in a charge transfer interaction that often leads to the formation of an exciplex with characteristic structureless emission.[1] The photochemistry and photophysics of such systems are especially rich when 1,2-diarylethenes are employed as the hydrocarbon partners. In such systems, exciplex formation is accompanied by diminished or enhanced trans−cis photoisomerization of the olefinic double bond which can also become involved in addition reactions. The consequences of interactions between the lowest excited singlet state of *trans*-stilbene and ground-state aliphatic amines have been investigated extensively.[2,3] Especially notable are the studies by Lewis and co-workers[3] that have also led to an exploration of the synthetic potential of intramolecular interactions of the styrene/amine[4] and stilbene/amine[5] partners.

In 1,2-diarylethenes with unsymmetrical aryl substituents, rotation about the essential aryl−vinyl single bond leads to an equilibrium mixture of distinct ground-state conformers. An excellent review of the photophysical manifestations of rotational isomerism in such molecules appeared recently,[6a] and earlier reviews are also available.[6b,7,8] Electronic excitation of such molecules often sufficiently reverses single/double bond order to convert freely equilibrating ground-state conformers into non-interconverting excited molecules with different structures and properties. When these molecules participate in charge-transfer interactions with appropriate quenchers, formation of distinct conformer-specific exciplexes is expected. Rotamerism has been studied most thoroughly in *trans*-1-(2-naphthyl)-2-phenylethene (NPE).[9−12] This paper presents a quantitative evaluation of the interaction of the lowest excited singlet states of NPE with tri-*n*-butylamine (TBA) in terms of the behavior of its two non-interconverting excited rotamers.

Experimental Section

Materials. Sources of *trans*-1-(2-naphthyl)-2-phenylethene and methylcyclohexane (MCH) were previously described.[12] Tri-*n*-butylamine (Aldrich, 99%) was distilled from mossy zinc under reduced pressure immediately before use.

Absorption and Fluorescence Spectra. Spectrophotometers employed in this work were previously described.[12] Fluorescence spectra

† Permanent address: Department of Chemistry, Florida International University, Miami, FL 33199.

⊗ Abstract published in *Advance ACS Abstracts,* August 1, 1996.

(1) See, e.g.: (a) Hui, M.-H.; Ware, W. R. *J. Am. Chem. Soc.* **1976**, *98*, 4718−4727. (b) Yang, N. C.; Shold, D. M.; Kim, B. *J. Am. Chem. Soc.* **1976**, *98*, 6587−6596. (c) Saltiel, J.; Townsend, D. E.; Watson, B. D.; Shannon, P.; Finson, S. L. *J. Am. Chem. Soc.* **1977**, *99*, 884−896.

(2) Kawanisi, M.; Matsunaga, K. *J. Chem. Soc., Chem. Commun.* **1972**, 313−314.

(3) (a) Lewis, F. D.; Ho, T.-I. *J. Am. Chem. Soc.* **1977**, *99*, 7991−7996. (b) Lewis, F. D.; Simpson, J. T. *J. Phys. Chem.* **1979**, *83*, 2015−2019. (c) Hub, W.; Schneider, S.; Dörr, F.; Oxman, J. D.; Lewis, F. D. *J. Am. Chem. Soc.* **1984**, *106*, 701−708. (d) Hub, W.; Schneider, S.; Dörr, F.; Oxman, J. D.; Lewis, F. D. *J. Am. Chem. Soc.* **1984**, *106*, 708−715. (e) Lewis, F. D. *Adv. Photochem.* **1986**, *13*, 165−235. (f) Lewis, F. D. *Acc. Chem. Res.* **1986**, *19*, 401−405.

(4) (a) Lewis, F. D.; Reddy, G. D.; Schneider, S.; Gahr, M. *J. Am. Chem. Soc.* **1989**, *111*, 6465- 6466. (b) Lewis, F. D.; Reddy, G. D.; Schneider, S.; Gahr, M. *J. Am. Chem. Soc.* **1991**, *113*, 3498−3506. (c) Lewis, F. D.; Reddy, G. D.; Bassani, D.; Schneider, S.; Gahr, M. *J. Photochem. Photobiol. A* **1992**, *65*, 205−220. (d) Lewis, F. D.; Reddy, G. D.; Bassani, D.; Schneider, S.; Gahr, M. *J. Am. Chem. Soc.* **1994**, *116*, 597−605.

(5) Lewis, F. D.; Bassani, D. M.; Burch, E. L.; Cohen, B. E.; Engleman, J. A.; Reddy, G. D.; Schneider, S.; Jaeger, W.; Gedeck, P.; Gahr, M. *J. Am. Chem. Soc.* **1995**, *117*, 660−669.

(6) (a) Mazzucato, U.; Momicchioli, F. *Chem. Rev.* **1991**, *91*, 1679−1719. (b) Mazzucato, U. *Pure Appl. Chem.* **1982**, *54*, 1705−1721.

(7) Scheck, Yu. B.; Kovalenko, N. P.; Alfimov, M. V. *J. Lumin.* **1977**, *15*, 157−168.

(8) (a) Fischer, E. *J. Photochem.* **1981**, *17*, 331−340. (b) Fischer, G.; Fischer, E. *J. Phys. Chem.* **1981**, *85*, 2611−2613.

(9) Haas, E.; Fischer, G.; Fischer, E. *J. Phys Chem.* **1978**, *82*, 1638−1643.

(10) Bartocci, G.; Masetti, F.; Mazzucato, U.; Marconi, G. J. *J. Chem. Soc., Faraday Trans. 2* **1984**, *80*, 1093−1105.

(11) (a) Birks, J. B.; Bartocci, G.; Aloisi, G. G.; Dellonte, S.; Barigelletti, F. *Chem. Phys.* **1980**, *51*, 113−120. (b) Bartocci, G.; Mazzucato, U.; Masetti, F.; Aloisi, G. G. *Chem. Phys.* **1986**, *101*, 461−466.

(12) Saltiel, J.; Sears, D. F., Jr.; Choi, J.-O.; Sun, Y. P.; Eaker, D. W. *J. Phys. Chem.* **1994**, *98*, 35−46 and references cited therein.

S0002-7863(96)01340-6 CCC: $12.00

were measured either in the flow cell system using Ar-outgassed solutions[12] or in degassed (five freeze−pump−thaw cycles) quartz cells. The temperature of fluorescence samples was maintained at 25.0 °C using a Neslab RTE-4DD refrigerated circulating bath and was monitored by means of an Omega Engineering Inc. Model 199P2 RTD digital thermometer equipped with a HYP-4RTD hypodermic probe.[12]

Results

Mathematical Procedures. Resolution of fluorescence spectral matrices, each limited to a single λ_{exc}, into monomer and exciplex mixture spectra was achieved by principal component analysis with self-modeling (PCA-SM) as previously described.[12] The Lawton and Sylvestre self-modeling procedure[13] succeeds in these two-component resolutions as monomer and exciplex spectra exhibit wide wavelength regions at the onset (monomer mixture) and tail (exciplex mixture) portions where each mixture component contributes uniquely.[14] The validity of these two-component treatments depends on the extent to which monomer and exciplex compositions at each λ_{exc} are fortuitously independent of [TBA].

When spectra at all λ_{exc} are treated together, PCA identifies a four-dimensional (4-D) coordinate system whose axes α, β, γ, and δ correspond to combination coefficients of the four orthonormal eigenvectors V_α, V_β, V_γ, and V_δ, respectively. Each experimental spectrum S_i is given by a point $(\alpha_i,\beta_i,\gamma_i,\delta_i)$ in this 4-D space that corresponds to a linear combination of the four eigenvectors

$$S_i = \alpha_i V_\alpha + \beta_i V_\beta + \gamma_i V_\gamma + \delta_i V_\delta \quad (1)$$

The normalization condition of the spectra in the matrix ensures that all such points must fall within an $\alpha,\beta,\gamma,\delta$ normalization tetrahedron defined by

$$\sum_{j=1}^{n} S_{ij} = \alpha \sum_{j=1}^{n} V_{\alpha j} + \beta \sum_{j=1}^{n} V_{\beta j} + \gamma \sum_{j=1}^{n} V_{\gamma j} + \delta \sum_{j=1}^{n} V_{\delta j} \quad (2)$$

The four apexes of the tetrahedron are the combination coefficients of the four pure component spectra, two of which, NPE_A and NPE_B, are known at 30.0 °C from previous work.[12] The four sides and six edges of the tetrahedron correspond to the four possible combinations of three-component mixtures and to the six possible combinations of two-component mixtures, respectively. PCA treatment of fluorescence spectra obtained in the absence of quencher defines two principal eigenvectors as previously described.[12] Least-squares fitting of the eigenvectors to the exciplex free portion (320−378 nm) of each spectrum obtained in the presence of TBA allows extrapolation of the monomer part (NBE_A/NPE_B) of the spectrum over the entire wavelength range. The difference between each experimental spectrum and the corresponding monomer spectrum generated from the monomer eigenvectors defines the pure exciplex part of the spectrum. This procedure projects each spectrum obtained in the presence of TBA first onto the monomer edge and then onto the exciplex edge of the tetrahedron. The four-component spectral matrix is effectively reduced to two two-component matrices, and the search for pure component combination coefficients is performed along two separate normalization lines.

Alternatively the search for the pure component combination coefficients can be performed by moving along the two-component edges of the tetrahedron in 4-D space. This procedure was employed in the preliminary part of this work in defining the pure exciplex fluorescence spectra E_A and E_B.[15] The exciplex edge of the tetrahedron is defined as a least-squares line through points corresponding to the pure exciplex portion of each spectrum. The procedure employed to achieve linear least-squares fitting in 4-D space will be demonstrated first in 3-D space, where it is more easily visualized. A line in 3-D space can be defined by a direction vector and a single point through which the vector must pass. Projections of a line in α,β,γ space onto two of the three Cartesian planes generates two slopes, s, that can be used to define the direction vector. For instance, if projected lines in the $\alpha\beta$ and $\alpha\gamma$ planes have slopes $s_{\alpha\beta}$ and $s_{\alpha\gamma}$, the direction vector is given by $(1,s_{\alpha\beta},s_{\alpha\gamma})$. Any point $(\alpha_i,\beta_i,\gamma_i)$ whose projections fall simultaneously and exactly on the least-squares lines in the two selected planes also fall exactly on the 3-D line and can be used in conjunction with the direction vector to define the line. Stepping along the line can commence at such a point by use of a set of parametric equations that are based on the two-coordinate plane slopes

$$\alpha = t + \alpha_i \quad (3a)$$

$$\beta = s_{\alpha\beta} t + \beta_i \quad (3b)$$

$$\gamma = s_{\alpha\gamma} t + \gamma_i \quad (3c)$$

where t is the stepping parameter.

Likewise, when a set of combination coefficients $(\alpha_i,\beta_i,\gamma_i,\delta_i)$ can be obtained that falls on a straight line in 4-D space, a direction vector can be based on the slopes of least-squares lines through the points projected on three of the coordinate planes. These slopes can be used as above to define the 4-D line as a set of four equations with a common stepping parameter. Although the choice of coordinate planes would be arbitrary if all data points fell exactly on the edge of the tetrahedron, some care must be exercised in performing least-squares fitting when points with significant deviations from the projected line are involved. Generally, projected lines with steep slopes should be avoided because the least-squares procedure employed in fitting a line through points on the α,β plane minimizes the value of $\sum(\beta - \beta_i)^2$. When changes in α_i values are much smaller than changes in β_i, a better fit is obtained if it is based on minimizing the value of $\sum(\alpha - \alpha_i)^2$. The usual least-squares procedure can be forced to this result by replacing (α_i,β_i) with (β_i,α_i). Parametric lines defining the monomer and exciplex edges of the tetrahedron can be defined in this way.[15]

NPE Fluorescence Spectra at Several λ_{exc} and [TBA]. A set of fluorescence spectra (320−650 nm in 1-nm increments) was obtained from eight degassed solutions of NPE (5.68×10^{-6} M) in MCH containing the following concentrations of TBA: [TBA] = 0, 0.0277, 0.0504, 0.100_7, 0.151_0, 0.201_5, 0.251_8, and 0.302_0 M. Complications due to possible photoreactions in the course of the measurements were minimized by recording a single spectrum for solutions containing TBA at each of the following λ_{exc}: 318, 333, 340, 347, and 355 nm. Duplicate spectra at these λ_{exc} were recorded for the solution with [TBA] = 0 for a total of 45 spectra. Pure solvent background spectra were employed for baseline correction. These corrections were satisfactory provided that the Rayleigh scattered-light peak from the solvent did not overlap the region of the fluorescence spectrum. The onset of spectra for longer λ_{exc} were further corrected for residual Rayleigh scattered-light distortion by employing the eigenvectors from a set of NPE spectra obtained at short λ_{exc}. This procedure has been

(13) Lawton, W. H.; Sylvestre, E. A. *Technometrics* **1971**, *13*, 617−633.

(14) Sun, Y.-P.; Sears, D. F., Jr.; Saltiel, J. *Anal. Chem.* **1987**, *59*, 2515−2519.

(15) Choi, J.-O. Ph.D. Dissertation, The Florida State University, Tallahassee, FL, 1992.

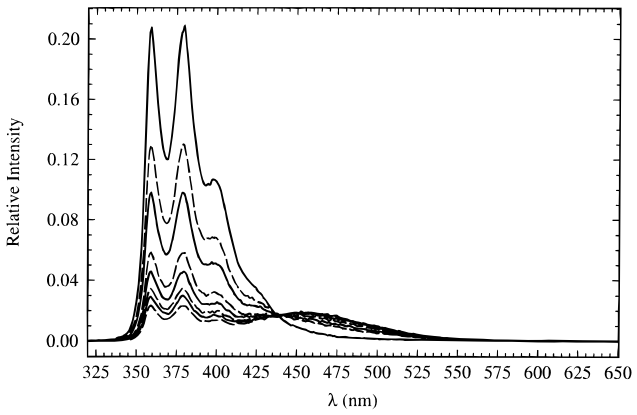

Figure 1. Effect of TBA on NPE fluorescence at 25 °C in MCH at $\lambda_{exc} = 355$ nm (see text for [TBA] values; the spectra are not corrected for nonlinearity in instrumental response).

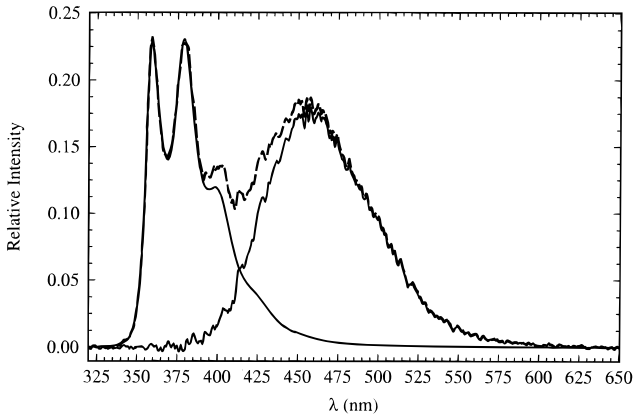

Figure 2. Spectrum for [TBA] = 0.302 M from Figure 1 resolved into composite monomer and exciplex contributions.

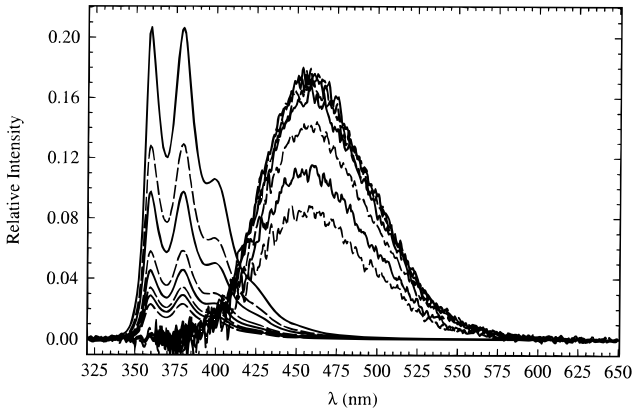

Figure 3. Monomer and exciplex (×10) contributions for the spectra in Figure 1.

previously described.[16] The set of background-corrected spectra for $\lambda_{exc} = 355$ nm is typical (Figure 1).

NPE_A and NPE_B Fluorescence Spectra. PCA on a matrix consisting of the 10 NPE fluorescence spectra in the absence of TBA gives two significant eigenvectors that allow the decomposition of spectra in the presence of TBA into monomer and exciplex parts by employing least-squares fitting (320−378 nm), as described in the Mathematical Procedures. The decomposition of a representative spectrum is shown in Figure 2. Deconvoluted monomer and exciplex spectra for $\lambda_{exc} = 355$ nm are shown as a function of [TBA] in Figure 3.

(16) Saltiel, J.; Zhang, Y.; Sears, Jr., D. F. *J. Am. Chem. Soc.* **1996**, *118*, 2811−2817.

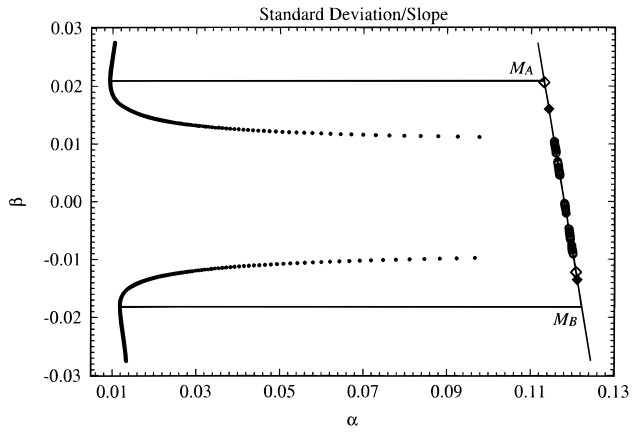

Figure 4. Normalization line and combination coefficients (○) for the NPE portions of fluorescence spectra for different λ_{exc} and [TBA]. The curves give the standard deviations of the global Stern−Volmer plots. Limits based on SV constants from the treatment of exciplex fluorescence (◇) and on the 30 °C spectra from ref 9 are also shown (◆).

The resolution of NPE_A and NPE_B spectra was achieved by applying the Stern−Volmer (SV) constant constraint[12] on a spectral matrix consisting of the monomer spectra for [TBA] = 0 and the decomposed monomer portions of all other spectra. Although all spectra were used in deriving the eigenvectors, spectra for [TBA] = 0.100_7 and 0.302_0 M were omitted from the SV optimization treatment. A TBA concentration error was suspected for the [TBA] = 0.100_7 M solution, and possible exciplex quenching by the amine could be operative at [TBA] = 0.302_0 M. The normalization line for this matrix is shown in Figure 4. As described earlier,[12] the SV constraint relies on the requirement that the correct resolution of monomer spectra should lead to λ_{exc}-independent SV constants, K_{SV}^A and K_{SV}^B. The location of the combination coefficients (α_A,β_A) of the fluorescence spectrum of NPE_A on the normalization line in Figure 4 is defined by minimizing the uncertainty in K_{SV}^B using

$$\frac{F^0(\beta^0 - \beta_A)}{F(\beta - \beta_A)} = 1 + K_{SV}^B[\mathrm{TBA}] \qquad (4)$$

where F^0 and F are areas of the fluorescence spectra (prior to normalization) and β_0 and β are coefficients of spectra for a specific λ_{exc} in the absence and in the presence of TBA.[12] Likewise, minimizing the uncertainty in K_{SV}^A defines the combination coefficients of NPE_B. To succeed the method requires that $K_{SV}^A \neq K_{SV}^B$. Standard deviations from the global SV lines are plotted as a function of β in Figure 4. The minima correspond to the global SV plots shown in Figure 5. The derived pure component fluorescence spectra of NPE_A and NPE_B are in very good agreement with those obtained earlier at 30 °C by using O_2 as the quencher.[12] They show somewhat better resolved vibrational structure, probably reflecting the 5 °C lower temperature (Figure 6).

E_A and E_B Fluorescence Spectra. PCA on a matrix consisting of the exciplex portions of the spectra as a function of λ_{exc} and [TBA], e.g. Figure 3, shows that it is a two-component system. Significant eigenvectors and the corresponding normalization line are shown in Figures 7 and 8, respectively. The locations of the combination coefficients for the two pure components on the normalization line are found on the basis of the premise that SV constants for exciplex formation should be λ_{exc}-independent (see eq 11 below). The resulting pure component exciplex spectra are shown in Figure 9. They are clearly consistent with the Lawton and Sylvestre non-negativity constraint.[13] As before, spectra for [TBA] =

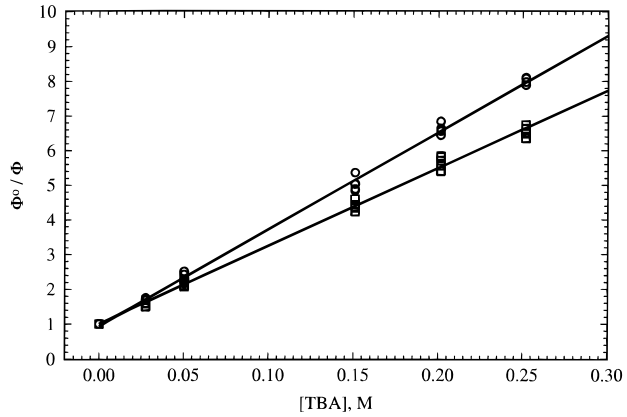

Figure 5. Global Stern−Volmer plots for TBA quenching of resolved NPE_A (□) and NPE_B (○) fluorescence in MCH at 25 °C.

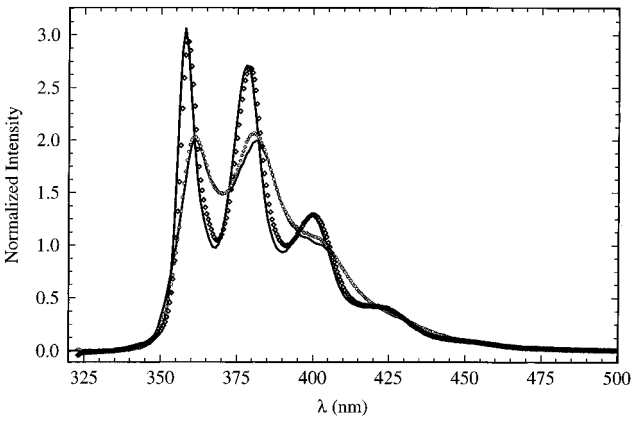

Figure 6. Pure component NPE_A (broad) and NPE_B (sharp) spectra for MCH at 25 °C based on the optimum SV limits in Figure 4. The points show the resolved spectra at 30 °C from ref 9 shifted 3 nm to the red to correct for an instrumental calibration error.

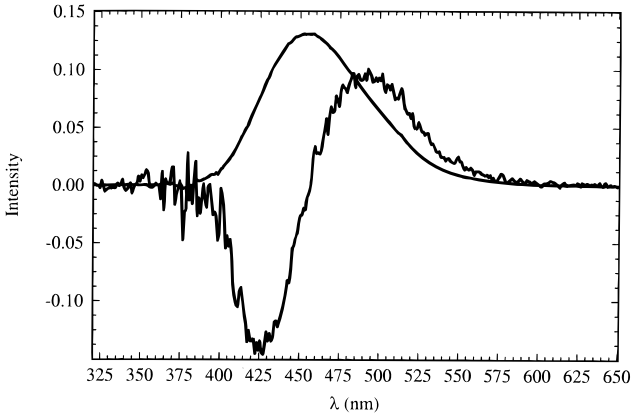

Figure 7. Significant eigenvectors from the matrix of resolved composite exciplex fluorescence spectra at different λ_{exc} and [TBA] in MCH at 25 °C. The four largest eigenvalues are 0.2960, 0.1188 × 10^{-2}, 0.9995 × 10^{-4}, and 0.4150 × 10^{-4}, respectively.

0.1007 M were not included in this analysis. Also excluded from this analysis were spectra for the highest [TBA] because of possible TBA quenching of exciplex emission at this concentration.

The Four-Component System. PCA was applied to a spectral matrix consisting of all experimental fluorescence spectra. Resulting significant eigenvectors and the corresponding eigenvalues for the four-component system are shown in Figure 10. Combination coefficients (α_i,β_i,γ_i,δ_i) for the decomposed monomer and exciplex parts of the spectra and for the pure component spectra derived in the preceding two

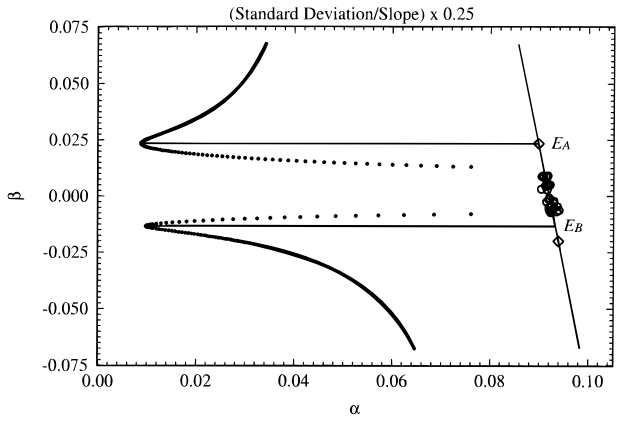

Figure 8. Normalization line based on the vectors in Figure 7 and combination coefficients (○) of the composite exciplex fluorescence spectra. The curves give the standard deviation of the global exciplex plots (eqs 11−14). Limits based on SV constants from the treatment of monomer fluorescence (◇) are also shown.

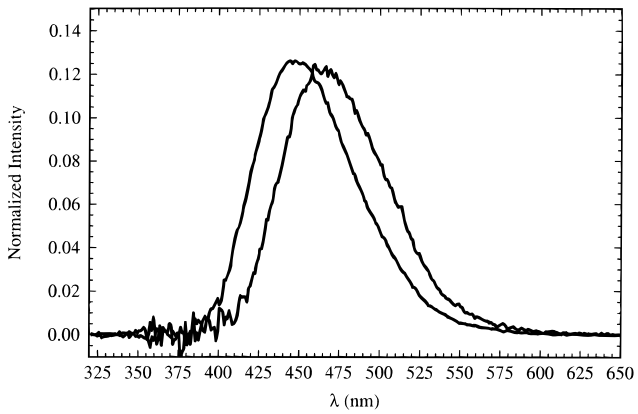

Figure 9. Pure component E_A (longer λ_{max}) and E_B spectra for MCH at 25 °C based on optimum fits to eq 11. The spectra are uncorrected for nonlinearity in instrumental response.

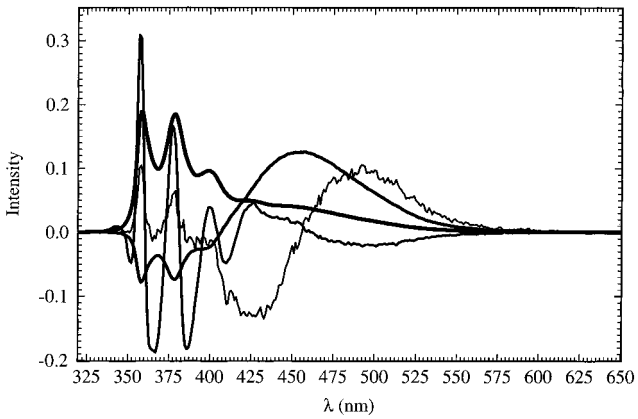

Figure 10. Significant eigenvectors from the global matrix consisting of all experimental fluorescence spectra and the resolved composite monomer and exciplex spectra. The six largest eigenvalues are 0.3820, 0.2891 × 10^{-1}, 0.1096 × 10^{-2}, 0.1158 × 10^{-3}, 0.3014 × 10^{-5}, and 0.2551 × 10^{-5}, respectively.

sections (Figures 6 and 9) were generated by taking dot products of these spectra with each of the four eigenvectors in Figure 10. The pure component combination coefficients define the corners of a tetrahedron in combination coefficient space, which is shown in (α,β,γ) space in Figure 11 [when (α,β,γ) is fixed, δ is defined by eq 2]. The tetrahedron is analogous to a 4-D phase diagram with the location of the combination coefficients of each spectrum giving the fractional contributions, x_{ij} (j =

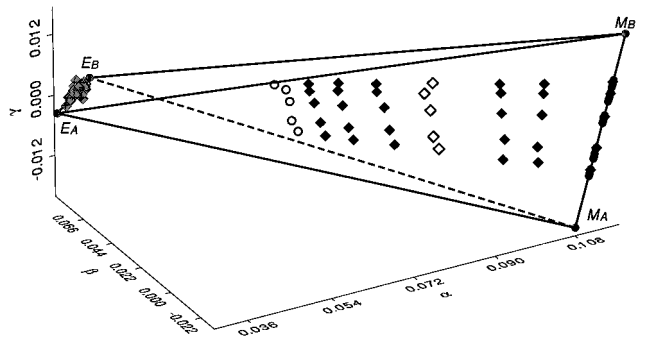

Figure 11. Combination coefficients for the four-component global matrix plotted in α,β,γ space. The figure shows the tetrahedron defined by the four pure component spectra (●). Combination coefficients for the experimental spectra used in the resolutions are designated by ◆; spectra designated ◇ and ○ were not used due to suspected [TBA] error and exciplex fluorescence quenching by TBA, respectively.

M_A, M_B, E_A, E_B, where M and E designate monomer and exciplex, respectively), of each pure component to the *i*th spectrum

$$S_i = x_{iM_A}S_{M_A} + x_{iM_B}S_{M_B} + x_{iE_A}S_{E_A} + x_{iE_B}S_{E_B} \qquad (5)$$

and

$$\begin{bmatrix}\alpha_i\\ \beta_i\\ \gamma_i\\ \delta_i\end{bmatrix} = \begin{bmatrix}\alpha_{M_A} & \beta_{M_A} & \gamma_{M_A} & \delta_{M_A}\\ \alpha_{M_B} & \beta_{M_B} & \gamma_{M_B} & \delta_{M_B}\\ \alpha_{E_A} & \beta_{E_A} & \gamma_{E_A} & \delta_{E_A}\\ \alpha_{E_B} & \beta_{E_B} & \gamma_{E_B} & \delta_{E_B}\end{bmatrix}\begin{bmatrix}x_{iM_A}\\ x_{iM_B}\\ x_{iE_A}\\ x_{iE_B}\end{bmatrix} \qquad (6)$$

Discussion

Effects of electron-donating amines, acting through charge-transfer interactions, on NPE fluorescence and trans → cis photoisomerization were first reported by Aloisi, Mazzucato, and co-workers.[17] SV constants for fluorescence quenching increased with a decrease in the ionization potential of the amine, and NPE-fluorescence quenching was accompanied by the appearance of exciplex fluorescence.[17] Enhanced photoisomerization was attributed to NPE triplet formation via exciplex intersystem crossing.[17] The possibility of differential NPE conformer behavior in such quenching interactions was first considered in a subsequent study by Das and co-workers.[18] The latter study included the system of the present investigation (NPE/TBA in Ar-outgassed MCH at unspecified ambient temperature). Evidence for conformer-specific quenching interactions was sought in the excitation, λ_{exc}, and monitoring wavelength, λ_{em}, dependencies of effective $\bar{K}_{SV}$ values (the bar designates a composite quantity reflecting the behavior of the mixture) and τ_e's, exciplex fluorescence lifetimes. Observed effects were, however, subtle. Specifically for NPE/TBA in MCH the effective $\bar{K}_{SV}$ (λ_{exc} = 330 nm) changed from 18.5 to 19.5 M^{-1} and the effective $\bar{K}_{SV}$ (λ_{exc} = 345 nm) changed from 17.0 to 19.8 M^{-1} on changing λ_{em} from 384 to 362 nm. While all these $\bar{K}_{SV}$ values are well within the ±15% experimental uncertainty, a much larger effect was claimed when an unspecified longer λ_{exc} was employed: $\bar{K}_{SV}$ = 10.5 M^{-1} for λ_{em} = 395 nm. Of greater significance was a shift of the exciplex fluorescence λ_{max} as λ_{exc} was changed to longer values: λ_{max} = 465 and 472 nm at λ_{exc} = 330 and 360 nm, respectively. The exciplex fluorescence lifetime, 21 ns for λ_{em} = 510−530 nm and [TBA] = 0.49 M, showed a systematic decrease of 10−15% on changing λ_{em} from 530 to 450 nm. While these observations were promising, they fell short of establishing conformer-specific $K_{SV}{}^i$ values and resolved exciplex fluorescence spectra. Subsequent studies on the interaction of related 1,2-diarylethenes singlet excited states with amines have also failed to yield intrinsic conformer properties.[19]

Our earliest attempt to apply PCA-SM on the fluorescence spectra of the NPE/TBA system in MCH[20] failed, in part, because it was based on an incorrect resolution of NPE_A and NPE_B fluorescence spectra.[12,21] A later attempt, based on the correct resolution of NPE_A and NPE_B fluorescence, succeeded in the resolution of the two pure exciplex fluorescence spectra, E_A and E_B, based on the Lawton and Sylvestre non-negativity constraints,[13] but resulted in an erroneous, complicated analysis of the dependence of the fluorescence quantum yields of the four components on [TBA].[15] That study employed the flow-cell system and Ar-outgassing and was flawed due to incomplete outgassing of the reference solution of NPE in the absence of TBA. The present study avoids complications due to adventitiously present O_2 by employing carefully degassed solutions. It succeeds in defining intrinsic conformer-specific rate constants for ^{1}NPE*/TBA interactions.

Mechanism and Kinetics Parameters. The strict adherence of NPE conformers to Havinga's NEER (nonequilibration of excited rotamers) principle[22] is firmly established.[6−8,12] The simplest mechanism that will account for the observations reported here is shown in Scheme 1. We adopt the Birks notation for the rate constants[23] such that subscripts m and e represent NPE monomer and (^{1}NPE*/TBA) exciplex and all other symbols have their usual meanings. The composite behavior of NPE fluorescence at a specific λ_{exc} as a function of [TBA] is given by

$$\frac{\bar{\phi}_f^{\circ}}{\bar{\phi}_f} = [\sum_i x_i(1 + K_{SV}{}^i[\mathrm{TBA}])^{-1}]^{-1} \qquad (7)$$

which is analogous to a previously derived expression.[18] The bars over the symbols in eq 7 again designate quantities that reflect the behavior of the conformer mixture, $K_{SV}{}^i = p_{ei}k_{ei}\tau_{mi}$ is the SV constant of the *i*th conformer where $p_{ei} = (1 + k_{-ei}\tau_{ei})^{-1}$ with $\tau_{ei} = (k_{fei} + k_{isei})^{-1}$ is the fraction of ^1E_i* that does not return to ^1M_i*. The fractional contribution of the *i*th conformer to the fluorescence, x_i, is given by

$$x_i = \frac{f_i\phi_{fmi}^{\circ}}{\bar{\phi}_{fm}^{\circ}} \qquad (8)$$

where $f_i = A_i/A$ is the excitation fraction of the *i*th conformer, ϕ_{fmi}° is its intrinsic fluorescence

$$\sum_i f_i\phi_{fmi}^{\circ} = \bar{\phi}_{fm}^{\circ} \qquad (9)$$

quantum yield in the absence of quencher, and $\bar{\phi}_{fmi}^{\circ}$ is the conformer mixture fluorescence quantum yield all at the

(17) (a) Aloisi, G. G.; Mazzucato, U.; Birks, J. B.; Minuti, L. *J. Am. Chem. Soc.* **1977**, *99*, 6340−6347. (b) Aloisi, G. G.; Bartocci, G.; Favaro, G.; Mazzucato, U. *J. Phys. Chem.* **1980**, *84*, 2020−2024.

(18) Wismontski-Knittel, T.; Sofer, I.; Das, P. K. *J. Phys. Chem.* **1983**, *87*, 1745−1752.

(19) See e.g.: (a) Aloisi, G. G.; Elisei, F. *J. Phys. Chem.* **1990**, *94*, 5813−5818. (b) Elisei, F.; Aloisi, G. G.; Mazzucato, U. *J. Phys. Chem.* **1990**, *94*, 5818−5823.

(20) Eaker, D. W. Ph. D. Dissertation, The Florida State University, Tallahassee, FL, 1984.

(21) Saltiel, J.; Eaker, D. W. *J. Am. Chem. Soc.* **1984**, *106*, 7624−7626.

(22) For a review. see: Jacobs, H. J.; Havinga, E. *Adv. Photochem.* **1979**, *11*, 305−373.

(23) Birks, J. B. *Photophysics of Aromatic Molecules*; Wiley: London, 1970.

Scheme 1

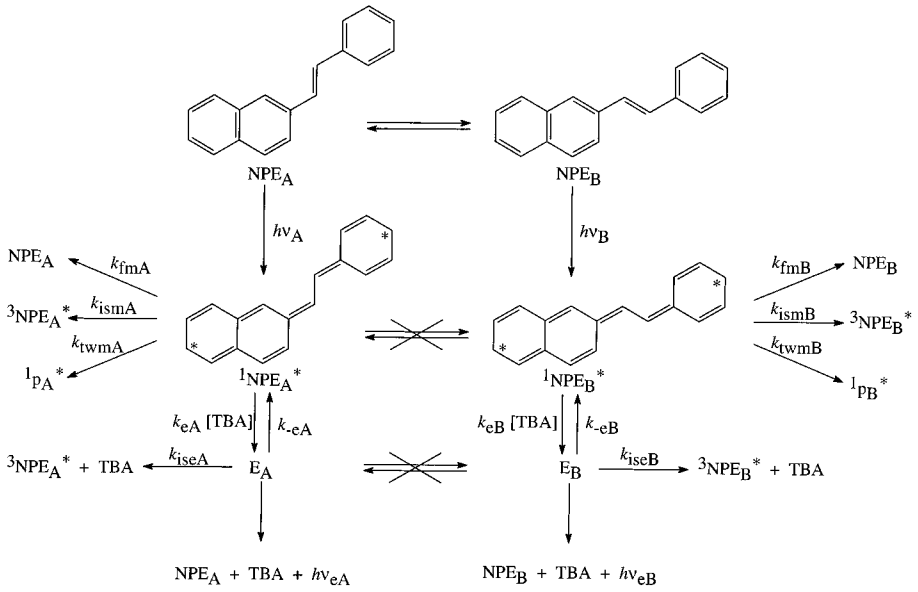

specified λ_{exc}. An attempt to derive x_i and $K_{SV}{}^i$ values for NPE from a nonlinear least-squares fit of quenching data to eq 7 failed even when applied to the fluorescence of a model mixture of anthracene and chrysene.[18,24] Recently, however, this method has been reported to succeed in another system.[26]

The successful resolution of the fluorescence spectra into their individual components provides the advantage of allowing application of simple kinetics expressions to the fluorescence of each component separately

$$\frac{\phi_{fmi}{}^{\circ}}{\phi_{fmi}} = 1 + K_{SV}{}^{i}[TBA] \tag{10}$$

$$\frac{1}{\phi_{fei}} = \frac{1}{\phi_{fei}{}^{\circ}}\left(1 + \frac{1}{K_{SV}{}^{i}[TBA]}\right) \tag{11}$$

where $\phi_{fei}{}^{\circ} = k_{fei}\tau_{ei}$ is the limiting fluorescence quantum yield of the *i*th exciplex at high [TBA], i.e., $K_{SV}{}^{i}[TBA] \gg 1$. In fact, it is this requirement that guides the PCA resolution of the spectra in the first place.

Pure Component Fluorescence Spectra. The success of the SV constraint in defining the combination coefficients of NPE_A and NPE_B fluorescence spectra (Figure 4) is a pleasant surprise. The earlier resolution was based on highly unselective essentially diffusion-controlled O_2 quenching, and consequently, the intrinsic pure conformer K_{SV} values differed by more than a factor of 5.[12] This large difference mirrors the difference in the fluorescence lifetimes ($\tau_{fma} = 3.4-3.7$ ns and $\tau_{fmB} = 19-24$ ns at room temperature[9] and $\tau_{fma} = 3.7-3.9$ ns and $\tau_{fmb} = 21.5-23.0$ ns in the 300−305 K range[10] have been reported in MCH for NPE_A and NPE_B, respectively) of the two conformers and leads to large changes in fractional contributions x_{ia} and x_{ib} with $[O_2]$. The corresponding large changes in β in eq 4 with $[O_2]$ make the SV constraint an especially sensitive criterion in defining the pure component combination coefficients. In the case of [TBA], however, the work of Das and co-workers[18] and our early observations[15,20] indicated very similar $K_{SV}{}^{i}$ values. Actually, the quencher-induced variation of the x_{ij} in eq 6 is so small that in our preliminary PCA treatment of NPE fluorescence spectra, obtained at constant λ_{exc} but with varying [TBA], the eigenvalues suggested two-component systems.[20] Only examination of the shapes of the third and fourth eigenvectors from such spectral matrices shows this conclusion to be less than valid. Nonetheless, these two-component treatments succeed in yielding resolved spectra corresponding to average mixtures of monomer and exciplex at each λ_{exc} based on the Lawton and Sylvestre non-negativity constraint. These solutions would be exact if $K_{SV}{}^{A} = K_{SV}{}^{B}$ were obeyed. The slope to intercept ratios of the global SV plots in Figure 5 give $K_{SV}{}^{A} = 22.2 \pm 1.2\ M^{-1}$ and $K_{SV}{}^{B} = 30.0 \pm 1.6\ M^{-1}$ that are surprisingly close in magnitude. Remarkably, a mere 26% difference in the K_{SV} values suffices for a successful spectral resolution based on the SV constant constraint (Figure 4).

On the basis of the mechanism in Scheme 1, the correct locations of the combination coefficients of E_A and E_B on the normalization line in Figure 8 should result in resolved areas of each exciplex as a function of [TBA] that adhere to eq 11 independent of λ_{exc}. Resolved exciplex fluorescence areas, F_{ei}, at each λ_{exc} were converted to fluorescence quantum yields by using NPE_A and NPE_B as standards

$$\phi_{fei} = \frac{x_{ei}F_{ei}}{x_{mi}{}^{\circ}F_{mi}{}^{\circ}}\phi_{fmi}{}^{\circ} \tag{12}$$

where

$$x_{mA}{}^{\circ} = \frac{\beta_{m}{}^{\circ} - \beta_{mB}}{\beta_{mA} - \beta_{mB}} \tag{13}$$

is the fractional contribution of $^1NPE_A$* fluorescence defined in Figure 4 at a specified λ_{exc} at [TBA] = 0, and

$$x_{eA} = \frac{\beta_{e} - \beta_{eB}}{\beta_{eA} - \beta_{eB}} \tag{14}$$

gives the fractional contribution of ^1E_A* fluorescence at the same λ_{exc} and at a specific [TBA]. The search for the pure component combination coefficients on the exciplex normalization line in Figure 8 is performed by stepping β_{eA} and β_{eB} in turn so as to minimize the standard deviation of global exciplex plots (Figure 12). Intercept to slope ratios of the optimum plots give $K_{SV}{}^{A}$

(24) The apparent quenching rate constants $p_{ei}k_{ei}$ are replaced by a more complex term when reversible electron transfer is explicitly included in the ^1M_i*/TBA encounter complex.[25]

(25) Indelli, M. T.; Scandola, F. *J. Am. Chem. Soc.* **1978**, *100*, 7733−7734.

(26) Burstein, E. A. *Photochem. Photobiol.* **1996**, *63*, 278−280.

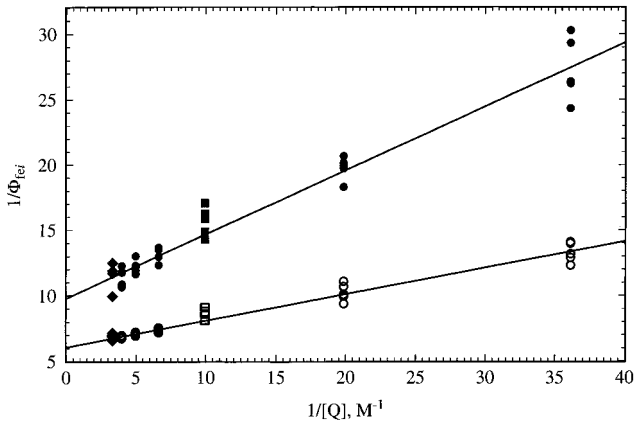

Figure 12. Global exciplex fluorescence plots based on eq 11: E_A (closed) and E_B (open) points define the upper and lower lines, respectively; points designated by squares and diamonds were not used in optimizing the fit to the lines (see text).

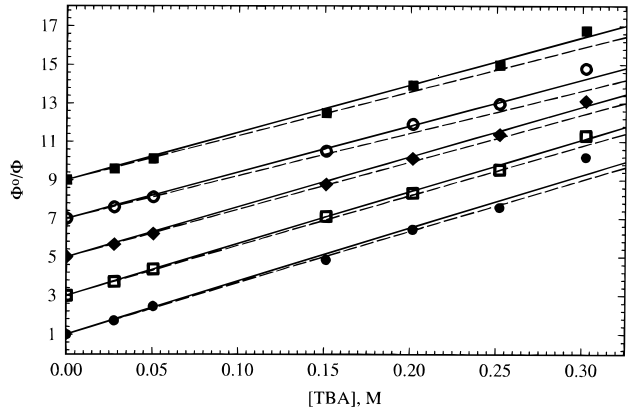

Figure 13. Composite SV plots for monomer fluorescence quenching at λ_{exc} 318 (●), 333 (□), 340 (◆), 347 (○), and 355 nm (■), respectively. Lines are calculated using eq 7 and K_{SV}'s from Figures 5 (—) and 12 (- - -), respectively.

$= 19.9 \pm 4.0\ M^{-1}$ and $K_{SV}^B = 30.1 \pm 4.3\ M^{-1}$ in excellent agreement with the values obtained from the monomer SV plots (Figure 5). Points for the highest [TBA] show small upward deviations from the global exciplex lines, hinting the onset of quenching of the exciplexes by TBA. Such quenching is a well-documented phenomenon for arene/amine systems.[1,3] Observations of diminished *trans*-stilbene/TBA exciplex ϕ_{fe} and τ_{fe} in benzene as [TBA] is increased to concentrations well in excess of those employed in our work are especially relevant.[3c]

An independent check of the self-consistency of the derived SV constants is afforded by eq 7. Since the x_i are known as a function of λ_{exc}, the K_{SV}^i values can be used to predict the [TBA] dependence of observed composite fluorescence quantum yields. The agreement between predicted and observed values is shown in Figure 13. It is especially gratifying at the longer λ_{exc} for which x_A is larger. The small systematic deviations of the points from the calculated line for $\lambda_{exc} = 318$ nm suggest either that our K_{SV}^B is somewhat overestimated or that a small error in λ_{exc} has resulted in an incorrect x_A for this wavelength. Improved agreement is obtained for $K_{SV}^B = 29.0\ M^{-1}$, a value well within our experimental uncertainty. However, the NPE_A fluorescence spectrum that is predicted if this K_{SV}^B value is chosen is inconsistent with the spectrum obtained at 30 °C.[12] The nearly parallel plots in Figure 13 illustrate the small range of effective $\bar{K}_{SV}$ values despite the considerable range in x_i. We also note that our $\bar{K}_{SV}$ values are substantially higher than those obtained earlier using Ar-outgassed solutions. It appears that more care should be exercised to ensure complete O_2 removal when this method is employed.[15,18,20]

Conformer Specific Reactivity. In the initial PCA resolution of NPE_A and NPE_B fluorescence spectra, the SV constraint was based on O_2 quenching of the fluorescence.[12] The choice of O_2 was dictated by the desire to maximize the (K_{SV}^B/K_{SV}^A) ratio in order to ensure the successful application of this constraint in defining the pure component combination coefficients. Since O_2 quenching is diffusion-controlled,[27] the large difference between the fluorescence lifetimes of the two conformers should be reflected fully in the SV constant ratio leading to highly differential quenching of the two emissions. Indeed, the resulting quenching rate constants, $k_{qox}^B = (3.51 \pm 0.24) \times 10^{10}\ M^{-1}\ s^{-1}$ and $k_{qox}^A = (3.50 \pm 0.23) \times 10^{10}\ M^{-1}\ s^{-1}$ in MCH at 30 °C are indistinguishable from each other and from the diffusion-controlled limit.[28] Although of key importance to the resolution of the pure conformer spectra, this initial determination of conformer specific bimolecular rate constants, involving a common quencher, yielded no secrets concerning the relative reactivity of the two conformers.

Formation of charge-transfer-stabilized singlet exciplexes is expected to be diffusion-controlled when electron transfer between the two partners in exergonic.[30] The early work of Aloisi, Mazzucato, Birks, and Minuti had established that NPE fluorescence is quenched much more efficiently by diethylaniline (DEA) than by tri-, di-, and monoalkylamines with higher ionization potentials.[17a] As expected, our initial measurements with DEA as quencher in MCH yielded λ_{exc}-dependent $\bar{K}_{SV}$ values that are significantly larger than those obtained for TBA: $\bar{K}_{SV}$ (λ_{exc}) of 75.5 M^{-1} (350 nm) and 134.6 M^{-1} (330 nm).[20] This accounts, in part, for the selection of TBA as the amine quencher in this work. Not only does its blue-shifted absorption spectrum, relative to DEA, allow for a wider λ_{exc} range to be employed in the NPE study, but the less than diffusion-controlled quenching of NPE conformer fluorescence affords the opportunity for differences in NPE_A and NPE_B reduction potentials to be reflected in the quenching rate constants.

On the basis of Scheme 1 and the average τ_{fmi} from ref 10, our SV constants give $p_{eA}k_{eA} = (5.8_4 \pm 0.3_2) \times 10^9\ M^{-1}\ s^{-1}$ and $p_{eB}k_{eB} = 1.35 \pm 0.08) \times 10^9\ M^{-1}\ s^{-1}$. It follows that TBA quenches $^1NPE_A$* 4.3 times more effectively than $^1NPE_B$*. This selectivity is due to the more favorable reduction potential of $^1NPE_A$* which is reflected in the larger red shift of its exciplex fluorescence. The relationship between the exciplex fluorescence energy at λ_{max} (or ν_e^{max}), $h\nu_e^{max}$, in *n*-hexane and one-electron polarographic donor oxidation and acceptor reduction potentials, E_D^{ox} and E_A^{red}, respectively, was established by the pioneering studies of Rehm and Weller.[31]

$$h\nu_e^{max} = E_D^{red} - E_A^{ox} - 0.10 \pm 0.08\ eV \qquad (15)$$

Since TBA is the common donor in our system, assuming

(27) For a review, see: Saltiel, J.; Atwater, B. W. *Adv. Photochem.* **1988**, *14*, 1−90.

(28) Adjustment for deviations from unity of SV plots in ref 9 have led to small changes in the SV constants that were reported there.[29]

(29) Saltiel, J.; Tarkalanov, N.; Sears, D. F., Jr. *J. Am. Chem. Soc.* **1995**, *117*, 5586−5587.

(30) (a) Rehm, D.; Weller, A. *Ber. Bunsen-Ges. Phys. Chem.* **1969**, *73*, 834−839. (b) Rehm, D.; Weller, A. *Isr. J. Chem.* **1970**, *8*, 259−271.

(31) (a) Rehm, D.; Weller, A. *Z. Phys. Chem. N. F.* **1970**, *69*, 183−200. (b) Rehm, D. *Z. Naturforsch.* **1970**, *25a*, 1441−1447. (c) Weller, A. *The Exciplex*; Gordon, M., Ware, W. R., Eds.; Academic Press: New York, 1975; pp 23−38.

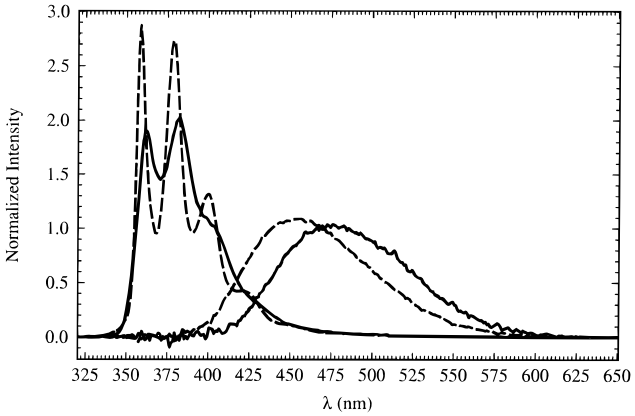

Figure 14. Resolved pure component NPE_A, NPE_B, E_A, and E_B fluorescence spectra corrected for nonlinearity in instrumental response.

identical Coulombic attraction in the two exciplexes gives

$$h\Delta\nu_e^{max} = -\Delta E_A^{red} \qquad (16)$$

where $h\Delta\nu_e^{max} = 2.9$ kcal/mol is defined by the shift in the λ_{max} (453 and 475 nm for ^1E_B* and ^1E_A*, respectively) of the resolved corrected exciplex fluorescence spectra in Figure 14 and ΔE_A^{red} is the reduction potential difference between the two conformers of NPE. It follows that the reduction potential of NPE_A is more favorable by 2.9 kcal/mol. Assuming that the exciplex is well represented as a contact radical-ion pair, the free energy change, ΔG_{et}, for the initial electron transfer step is given by the Weller equation[30]

$$\Delta G_{et} = E_D^{ox} - E_A^{red} - E_S - \frac{e_0^2}{\epsilon a} \qquad (17)$$

where E_S is the singlet energy of the excited partner and $e_0^2/\epsilon a$ is the Coulombic attraction term that accounts for free energy gain when $A^{\bullet-}$ and $D^{\bullet+}$ are brought to within encounter distance a in a solvent with dielectric constant ϵ. Again neglecting possible small differences in the Coulombic attraction term, it follows that

$$\Delta G_{et}^B - \Delta G_{et}^A = -\Delta E_A^{red} - \Delta E_S \qquad (18)$$

where $\Delta E_S = 0.77$ kcal/mol can be estimated from the positions of the 0−0 bands in the resolved fluorescence spectra of $^1NPE_A$* and $^1NPE_B$* (Figure 14). Accordingly, the change of the free energy for electron transfer to $^1NPE_A$* is more favorable by 2.1 kcal/mol than for electron transfer to $^1NPE_B$*. Neglecting the unknown difference between p_{eA} and p_{eB}, the observed more effective quenching of $^1NPE_A$* by TBA, corresponds to $\Delta G_e^{\ddagger B} - \Delta G_{et}^{\ddagger A} = 0.87$ kcal/mol. Thus a more favorable free energy for electron transfer of 2.1 kcal/mol is reflected in a more favorable free energy of activation for electron transfer of ∼0.9 kcal/mol.

Exciplex Fluorescence Quantum Yields. Composite fluorescence quantum yields, $\bar{\phi}_{fm}$, of NPE measured as a function of λ_{exc} in *n*-hexane[10,11] at 20 °C and in MCH[12] at 30 °C have been used together with $f_i(\lambda_{exc})$ and $x_i(\lambda_{exc})$ to determine pure component NPE_A and NPE_B fluorescence quantum yields.[12] Nearly identical values were obtained under these different conditions: $\phi_{fmA}^\circ = 0.60$ and 0.61 and $\phi_{fmB}^\circ = 0.83$ and 0.76 in *n*-hexane and MCH, respectively.[12] On the basis of the temperature dependence of $\bar{\phi}_{fm}$ at 316 and 355 nm,[12] we estimate $\phi_{fmA}^\circ = 0.63$ and $\phi_{fmB}^\circ = 0.79$ at 25 °C in MCH. These pure component quantum yields were used in eq 12 and in eq 16 with the x_{mi} at [TBA] = 0 to obtain

$$\frac{1}{\bar{\phi}_{fm(\lambda_{exc})}} = \frac{1}{\phi_{fmB}} + \left(\frac{1}{\phi_{fmA}} - \frac{1}{\phi_{fmB}}\right) x_{mA}(\lambda_{exc}) \qquad (19)$$

$\bar{\phi}_{fm}^\circ$ values at each λ_{exc} employed in this study.[12] Total fluorescence quantum yields were based on these $\bar{\phi}_{fm}^\circ$ values and on the relative areas of the fluorescence spectra (corrected for nonlinearity of instrumental response) in Table SI (deposited as supporting information). On the basis of eq 11, the inverse of the intercepts in Figure 12 gives $\phi_{feA}^\circ = 0.152 \pm 0.004$ and $\phi_{feB}^\circ = 0.210 \pm 0.004$. The exciplex fluorescence lifetime has been measured for [TBA] = 0.49 M and may have been subject to some self-quenching by the amine.[18] Accordingly, we regard the reported $\tau_{fe} = 21$ ns as a lower limit. The 10−15% drop in this lifetime as the monitoring wavelength is changed from 530 to 450 nm[18] suggests that the lifetime of E_A is somewhat longer than the lifetime of E_B. It follows that $k_{feA} \simeq k_{feB} \leq 1 \times 10^7$ s^{-1} (this estimate neglects the possible coupling of monomer and exciplex lifetimes that would result if exciplex formation were freely reversible). The importance of exciplex intersystem crossing in our system was not evaluated. Estimates of ϕ_{ise} in related systems, based on enhanced isomerization quantum yields associated with amine quenching of olefin fluorescence,[3,17] indicate that these can be substantial, but that their magnitude depends on the identities of the olefin, the amine, and the solvent.

Acknowledgment. This research was supported by NSF, most recently by Grant No. CHE 93-12918.

Supporting Information Available: A table of composite fluorescence quantum yields, $\bar{\phi}_f$, and fractional contributions, *x*, based on Figure 11, as a function of λ_{exc} and [TBA] (Table SI) (2 pages). See any current masthead page for ordering and Internet access instructions.

JA961340G